ELSEVIER

Hearing Research 92 (1995) 1–16

HEARING RESEARCH

Nonlinear effects of noise on phase-locked cochlear-nerve responses to sinusoidal stimuli

Edwin R. Lewis [a,*], Kenneth R. Henry [b]

[a] *Department of EECS, University of California, Berkeley, CA 9472, USA*
[b] *Department of Psychology, University of California, Davis, CA 9561, USA*

Received 18 June 1994; revised 25 July 1995; accepted 31 July 1995

Abstract

It is well known that, in a cochlear afferent axon with background spike activity, a sinusoidal stimulus (tone) of sufficiently low frequency will produce periodic modulation of the instantaneous spike rate, the alternating half cycles of which comprise excursions above and below the mean background spike rate. It also is known that if the amplitude of the stimulus is sufficiently small, the instantaneous spike rate follows very nearly a sinusoidal trajectory through these positive and negative excursions. For such cases, we define the AC responsiveness of a primary auditory afferent axon to be the amplitude of sinusoidal modulation of the instantaneous spike rate divided by the amplitude of the tone producing that modulation. In the experiments described in this paper, changes in AC responsiveness were followed during and after sudden changes in the background noise level. When the amplitude of the tone was sufficiently small relative to that of the noise, we found that the AC responsiveness can be strongly dependent on the time elapsed since the last change in noise level, while being nearly independent of the amplitude of the tone itself. Under those circumstances, after transitions between noise levels 20 dB apart, we observed changes in AC responsiveness that consistently followed time courses similar to those of the short-term mean (background) spike rate (approximating the adapting response to the noise alone), unfolding over several milliseconds or tens of milliseconds. At the time of the transition between noise levels, there was another change in AC responsiveness, which appeared to be instantaneous; as the noise level increased, the AC responsiveness immediately increased with it. This seemingly paradoxical effect and the similarity of the time courses of AC responsiveness and short-term mean spike rate both are consistent with a simple, descriptive model of spike generation involving the shifting of threshold along a bell curve.

Keywords: Adaptation; AC responsiveness; Slow nonlinearity; Instantaneous nonlinearity

1. Introduction

In mammalian cochlear nerve fibers, various degrees of phase locking have been observed in response to sinusoidal stimuli (tones) at frequencies up to approximately 5 kHz (Anderson et al., 1970; Palmer and Russell, 1986). At such high frequencies, a single cochlear axon produces at most 1 spike during any cycle (period) of the stimulus sine wave, and cannot produce a spike during every cycle. In fact, such an axon typically produces spikes at an average rate less than 100 spikes/s, or 1 spike for every 50 cycles at 5 kHz. Nevertheless, the axon can be capable of showing consistent phase preferences in the cycles in which it does fire. One can interpret this phase preference as modulation of the probability of firing, phase-by-phase during each cycle of the stimulus sine wave. Thus, for a 2 kHz tone, one would envision a 2 kHz AC variation in the firing probability. The amplitude and phase of such an AC component relative to the sinusoidal stimulus producing it will reflect the physical properties and the signal-processing properties of the sensory path from the outer ear canal to the cochlear nerve fiber. Included in the path is the spike generation process which is inherently nonlinear. In spite of this and other nonlinearities in the path, however, for an acoustic stimulus of sufficiently small amplitude one expects the relationship between the firing probability and the stimulus waveform to be approximated well by an affine function (i.e., by the first two terms of the Taylor series (e.g., see Selby, 1975, p. 601, or any calculus text) describing the complete nonlinear relationship).

* Corresponding author. Tel.: (510) 642-5169; Fax: (510) 643-6103.

SSDI 0378-5955(95)00189-1

Whereas a spike unfolds over a finite interval of time (several hundred microseconds in the case of the mammalian auditory nerve), in digital statistical analyses such as those applied in this paper, the firing of an axon usually is treated as an instantaneous event in discrete time (e.g., see Perkel et al., 1967). The translation from spike waveform to instantaneous event is accomplished by applying a slope-sensitive threshold to the waveform. The discrete time interval during which the waveform crosses the threshold in the designated direction is taken to be the instant of firing (spike onset). If one imagines that firing is a random process with probability density p, that the parameters of the system remain constant and that no stimulus is being applied so that p is constant, then

$$E[\textit{spike onsets}; t, t+\Delta t] = p\Delta t \tag{1}$$

where E [*spike onsets*; t, $t+\Delta t$] is the expected number of spike onsets in the time interval between t and $t+\Delta t$. Because the dimension of p is spike onsets/time, it often is called the instantaneous spike rate, and it is a standard measure of probability of firing. The model implied by Eq. 1 is a Poisson process. Although the spike-onset statistics of auditory-nerve fibers typically differ systematically from those of a Poisson process (both for short times, where the finite spike width and refractoriness come into play, and for long times, where fluctuations in excitability come into play), as long as instantaneous spike rates remain moderate (e.g., < 100 spikes/s) that model is sufficiently close to what actually occurs to serve our purpose here, namely qualitative understanding (e.g., Siebert, 1968; de Boer and de Jongh, 1978; Young and Barta, 1986; Winslow and Sachs, 1988, Teich et al., 1991; Edwards and Wakefield, 1993). As we mentioned in the previous paragraph, one would expect the relationship between p and a small-amplitude stimulus to be approximated well by an affine function. Thus, if the stimulus waveform were described by

$$S(t) = C\sin(\omega_0 t) \tag{2}$$

where the amplitude C is very small, then p should be a function of time, approximated well by

$$p(t) = A\sin(\omega_0 t + \theta) + B \tag{3}$$

where B is the background spike rate; and $\omega_0 = 2\pi f_0$, f_0 being the frequency of the stimulus sine wave given in Hz. If the parameters of the system remain constant, then, A, B and θ will be constant and A and θ can be estimated by observation of the correlation between spike generation and the stimulus waveform.

Computation of the correlation often is carried out with a period histogram, in which successive bins represent successive time increments over the period of the stimulus sine wave (Goldberg and Brown, 1969; Anderson et al., 1970; Johnson, 1978). If bin number 1 begins at $t = 0$, then under the assumption that the parameters of the system remain constant, the period histogram can be translated to a succession of discrete estimates of $p(t)$ as follows:

$$\lim X_i/N|_{N\to\infty} = \int_{t=(i-1)\tau}^{i\tau} p(t)\,dt \approx \tau p(t)|_{t=(i-1/2)\tau}$$

$$p(t)|_{t=(i-1/2)\tau} \approx \frac{X_i}{N\tau} \tag{4}$$

where X_i is the number of spikes accumulated in bin i; N is the total number of stimulus sine-wave cycles sampled; τ is the time increment represented by each bin during each cycle. The commonly used measure of correlation is the vector strength, r (Goldberg and Brown, 1969):

$$r = \frac{\sqrt{\alpha^2+\beta^2}}{n}$$

$$\alpha = \sum_{i=1}^{m} X_i \cos\left(\frac{2\pi i}{m}\right)$$

$$\beta = \sum_{i=1}^{m} X_i \sin\left(\frac{2\pi i}{m}\right) \tag{5}$$

where m is the number of bins in the histogram (each representing a phase range of $2\pi/m$ rad of the stimulus sine-wave cycle), and n is the total number of spikes in the histogram. When $p(t)$ is approximated well by Eq. 3, with $A < B$ (keeping the instantaneous spike rate greater than zero), then

$$A = 2\frac{nr}{Nm\tau}$$

$$B = \frac{n}{Nm\tau}$$

$$\theta = \tan^{-1}\left[\frac{\beta}{\alpha}\right] \tag{6}$$

Some hearing researchers have used vector strength as a basis for estimating the tuning properties of the cochlea and other vertebrate auditory organs (e.g., Johnson, 1980; Narins and Hillery, 1983). Others have examined the steady-state effects of interfering stimuli on vector strength computed for a given sine wave (e.g., the effect of a 4 kHz tone on r computed for a 1 kHz tone when both tones are presented together) (Javel, 1981; Greenwood, 1986). In this paper we describe a project in which we attempted to carry out a qualitative survey of nonlinear effects of broad-band background stimuli (acoustic noise) on the responsiveness of the ear to tones. For this purpose, we elected to use A (the amplitude of the AC modulation of the instantaneous spike rate) rather than r. Any change in A in response to a background stimulus not correlated with the tone for which A is computed is, by definition of linearity, a nonlinear effect (see Discussion). Because hearing is a dynamic process, in which temporal cues are important, we were especially interested in observing the nonlinear effects dynamically rather than in steady state.

The work reported here should be considered an extension of that of Abbas (1981). It is complementary to that of Costalupes (1985), that of Narins and colleagues (e.g., Narins and Wagner, 1989), and that of Simmons and colleagues (e.g., Freedman et al., 1988), all of which dealt with steady-state observations.

2. Methods

The gerbil preparation used in this project was the same as that described previously (Lewis and Henry, 1989). The bulla was opened and the auditory nerve was exposed under the floor of the round-window antrum. Each axon studied was impaled by a glass micropipette electrode, filled with 3.0 M NaCl and having resistance greater than 50 MΩ. Auditory stimuli were applied through a closed-field system comprising an Etymotic ER-2 driver and a Etymotic ER-10 low-noise microphone sealed to the external auditory canal. Cochlear axons were identified by their response to periodic noise bursts. Tone bursts were used to estimate best frequency (BF) and threshold at estimated BF. A tone burst at estimated BF and having a fast rise time was used to estimate response latency. A unit was identified as being a primary afferent axon by virtue of its response latency (< 2.0 ms), the depth at which it was penetrated (< 500 μm from the surface of the auditory nerve), and the primary-type patterns of its responses to tone bursts at BF. Experiments were carried out on 58 units from 9 gerbils. Estimated BFs ranged from 800 Hz to 11.5 kHz.

As a sinusoidal stimulus to generate phase locking, we selected a tone with a frequency (typically 1.0 kHz) that was high enough to allow us to follow rapid changes in A (from one sine-wave cycle to the next), but low enough to allow the instantaneous spike rate (instantaneous probability of firing) to follow the sine wave, phase-by-phase within each cycle. The sine wave was generated digitally and was presented as periodic tone bursts with trapezoidally modulated amplitude (1.0 cycle rise and fall times). The phase of the sine wave was fixed relative to the trapezoidal envelope. The noise waveform was produced by a General Radio Gaussian White Noise Generator (Model 1390-B) and was shaped by a 1/3-octave equalizer to produce nearly flat power spectral density (± 3 dB from 300 Hz to 10 kHz, with spectral analysis at 37.5 Hz bandwidth) of the acoustic output of the ER-2, as sensed by the ER-10, and analyzed by a Hewlett-Packard 3561A Dynamic Signal Analyzer. The noise also was presented as periodic bursts, sometimes superimposed on background noise. The envelope of each noise burst was trapezoidal (1.0-ms rise and fall times); and the onset of the noise burst occurred at a fixed time relative to the onset of the tone burst. The combined (noise and tone) stimulus patterns that we used are depicted in Fig. 1. Spikes, stimulus (as measured by the ER-10), and trigger signal (synchronized with respect to the onset of the tone burst) were recorded on separate channels of a TASCAM 234 4-channel cassette recorder (frequency range: 20 Hz to 20 kHz; dynamic range: 75 dB). The fourth channel was used for voice records. Spike onsets and trigger-signal onsets were detected off-line (i.e., from the tape) with lab-built electronic circuits. Detection of multiple firings from a single spike waveform was avoided by following each detected spike onset with a dead-time during which no further spike onsets could be detected. During the detection process, the recorded spikes and detected spike onsets (represented as pulses) were displayed simultaneously in parallel traces on a multitrace analog cathode-ray oscilloscope so that the observer could adjust the threshold and dead-time of the detector circuit until each detected onset corresponded to 1 spike and every spike was represented by one detected onset. Relative times of trigger onsets and spike onsets were measured with a digital clock (with 1.0 μs resolution). To estimate the phase-locked response to the tone, we converted these data to peristimulus time histograms (PSTHs) with bin width τ (typically 1/12 ms for a 1.0 kHz tone), taken over N (typically 1000 or more) repetitions of the combined tone and noise bursts. The range of the abscissa for a period histogram normally is 1 cycle of the stimulus sine wave; and the displayed spike counts normally have been accumulated over many presentations of the cycle, presumably under identical conditions. The range of the abscissa of our PSTHs always spanned many cycles of our stimulus sine wave, successive cycles within the PSTH having been presented under different conditions (i.e., at different times relative to the beginning of the

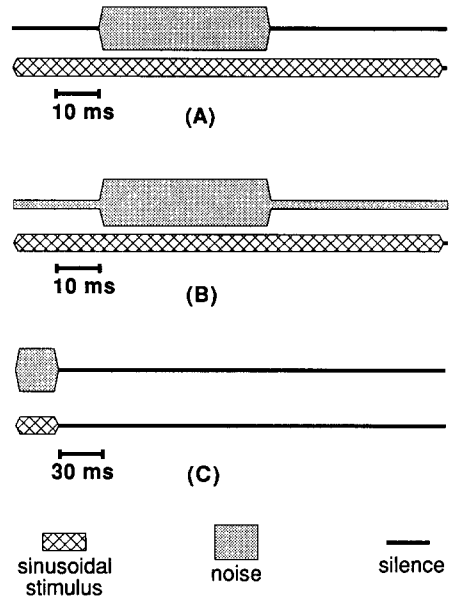

Fig. 1. Three stimulus patterns used in the experiments reported here. Each line shows a full stimulus period. In (B), the pattern used for most units, the background noise was continuous and the noise amplitude increased by 20 dB during the trapezoidal burst. The detailed temporal parameters of these patterns are given in Section 2.

noise burst). Dividing the spike count in each bin by $N\tau$ converts it to an estimate of instantaneous spike rate ($p(t)$ in Eq. 4). Thus, from these PSTHs, we related the instantaneous spike rate to the phase of the sine wave *and* to the time relative to the beginning of the noise burst.

The amplitude (A) of the AC modulation of the instantaneous spike rate in response to the tone could be estimated by means of Eqs. 5 and 6. Equivalently, it could be estimated by computing the maximum discrete cross-correlation between a sine wave at the stimulus frequency and the instantaneous spike rate. Because the sinusoidal modulation of instantaneous spike rate usually was conspicuous in our PSTHs, we preferred carrying out the computations in a spread-sheet format, so that we could visualize the process on a cycle-by-cycle basis and thus be confident that our computational algorithms were not generating artifacts. For us, visualization was easier with the cross-correlation method, which allowed us to see the phase match between the modulated spike rate and the maximally correlated sine wave. The computation was carried out as follows:

$$\langle A \rangle = \frac{2}{N\tau Km} \sum_{i=1}^{Km} X_i \sin\left[\frac{(b+2i)\pi}{m}\right] \tag{7}$$

where $\langle A \rangle$ is the average value of A taken over the PSTH segment being analyzed; N is the number of repetitions of the noise burst; τ is the time represented by each histogram bin; X_i is the number of spikes in bin i; m is the number of bins per cycle of the sinusoidal stimulus; K is an integer (the number of periods of the sinusoidal stimulus covered by the PSTH segment being analyzed). $\langle A \rangle$ was calculated for each of $2m$ steps of phase (b ranging in integral steps from 0 to $2m-1$), and the value of phase yielding the largest positive value of $\langle A \rangle$ was selected. In that case,

$$\theta \approx \frac{b\pi}{m} rad \tag{8}$$

B was computed as follows:

$$\langle B \rangle = \frac{1}{N\tau Km} \sum_{i=1}^{Km} X_i \tag{9}$$

where $\langle B \rangle$ is the average value of B taken over the PSTH segment being analyzed.

In order to satisfy the requirement that $A < B$, and thus avoid introduction of a saturation artifact (clipping) in our computation of A, we required three things: (1) that the axon have a substantial mean background spike rate in the absence of the tone, (2) that the amplitude of the tone not be so large as to drive the probability of firing close to zero for any bin (e.g., in the trough of the AC modulation of instantaneous spike rate), and (3) that the total number of spikes sampled be large enough compared with the number of histogram bins to insure that the expected number of spikes per bin be considerably greater than zero throughout the histogram. When the noise amplitude was large (during the noise burst), the noise itself elicited the required background firing rate. The lab-generated PSTH software that we used provided a time window having an adjustable width and position. Each PSTH comprised a 300-bin sampling over the designated window. Our algorithm (Eq. 7) for estimating the amplitude of the AC modulation of instantaneous spike rate required that we use a window duration that gave precisely an even integral number of bins per cycle of the sinusoidal stimulus, and the total number of spikes sampled typically was large enough to allow us to use 12 bins per cycle of the stimulus sine wave without clipping in the troughs. To enhance visualization of the AC modulation of instantaneous spike rate, PSTHs occasionally were smoothed through a succession of one or more discrete convolutions with a simple 3-bin smoothing function (0.25, 0.5, 0.25). The correlation operation in Eq. 7, however, always was carried out on the unsmoothed histogram.

If $A < B$ and if the system were responding linearly to the tone, then the following should be true: A (the amplitude of the AC modulation of instantaneous spike rate) should be directly proportional to C (the amplitude of the sinusoidal stimulus); B (the short-term mean spike rate) should be independent of C [1]; and θ (the phase of the AC modulation of instantaneous spike rate) should be independent of C. One expects B to depend on the amplitude of the noise stimulus. On the other hand, any dependence of A or θ on the amplitude of the noise stimulus will imply nonlinear effects of that stimulus on the AC responsiveness of the system. One class of such effects, labelled synchrony suppression, already has been well studied (Javel, 1981; Greenwood, 1986). The focus of this paper will be elsewhere. Our experimental paradigm is very similar to that employed by Abbas (1981), the principal differences being our use largely of noise bursts during a nearly continuous tone (stimulus patterns A and B) and our focus on keeping $A < B$.

3. Results

Stimulus pattern B was applied to most of the units in the study. The PSTHs of Fig. 2 are representative of those taken during the noise burst in that stimulus pattern. The unit in this case had a characteristic frequency (CF) of 3 kHz, with a threshold at CF of approximately 20 dB SPL. The RMS noise amplitude during the burst was 74 dB SPL (9700 Hz bandwidth). The PSTHs show primary-type re-

[1] Some previous studies of the effects of noise on cochlear responses to tones have been based on the dependence of B on C (rate responses or DC responses), reflecting a nonlinear process akin to rectification (e.g., Costalupes et al., 1984; Costalupes, 1985; Narins, 1987; Erell, 1988; Dolan and Nuttall, 1989).

sponse with conspicuous adaptation during the noise burst. For Fig. 2A and B, respectively, the RMS amplitudes of the 1.0 kHz stimuli were 60 and 70 dB SPL. Both histograms have been convolved once with the 3-bin smoothing function. AC modulation of instantaneous spike rate is clear in Fig. 2B but not as obvious in Fig. 2A. Analyses of the unsmoothed histograms with the algorithm of Eq. 7, taken over the first 25 ms of the noise burst, led to the correlation functions shown in Fig. 3A, in which $\langle A \rangle$ is plotted against discrete phase, b. Note that the phases of the correlation functions are virtually identical, implying the phase of the AC response relative to the sinusoidal stimulus was independent of the amplitude of that stimulus (over the range from 60 to 70 dB SPL). Note also that the ratio of the peak amplitude (54.3 sp/s) of $\langle A \rangle$ computed for 70 dB SPL to that (18.1 sp/s) computed for 60 dB SPL is 9.54 dB (extremely close to the 10 dB stimulus amplitude ratio). Both of these observations imply that the system is responding nearly linearly to these tones.

Fig. 4A shows the AC responsiveness (measured as the transfer ratio $\langle A \rangle / C$, the average peak AC modulation of instantaneous spike rate divided the peak amplitude of the tone) computed over successive 5-ms segments of the PSTHs in Fig. 2A,B, beginning at the time of onset of the

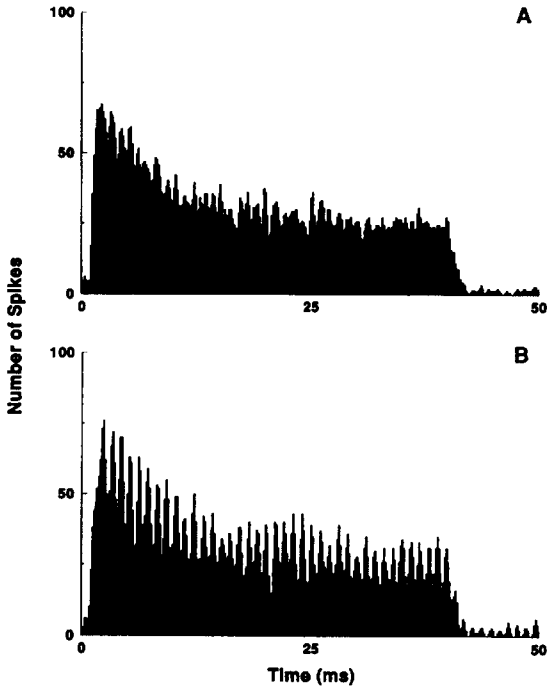

Fig. 2. PSTHs for a 3 kHz unit, taken over a 50-ms segment of the 101-ms noise cycle of stimulus pattern B. The PSTHs cover the entire response to the 40-ms noise burst. The frequency of the tone was 1 kHz. The background noise amplitude was 54 dB SPL and the amplitude of the noise burst was 74 dB SPL (each taken over the entire 9700 Hz bandwidth of the noise). Both PSTHs were taken over 170-s sampling periods, and both were smoothed by single convolution with the 3-bin function described in Section 2. Amplitudes of the tone were 60 and 70 db SPL for A and B, respectively.

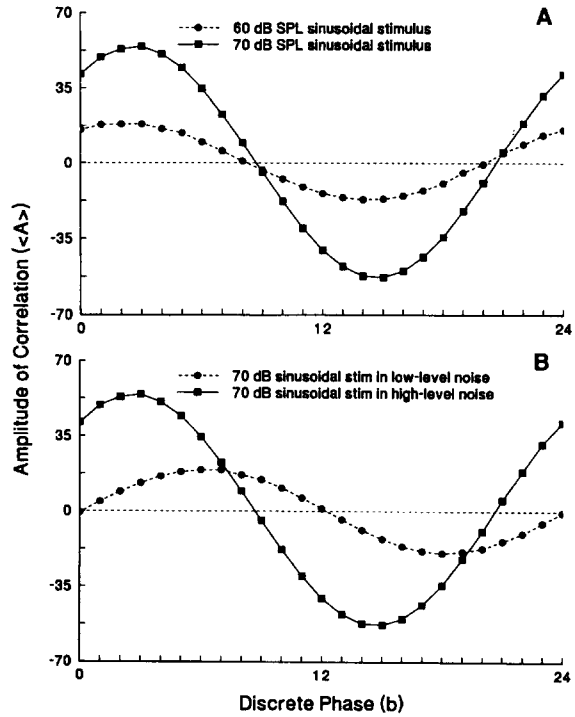

Fig. 3. Correlation functions (Eq. 7) computed over segments of unsmoothed PSTHs for the 3.0 kHz unit of Fig. 2 (again stimulus pattern B with 1 kHz tone; background noise amplitude: 54 dB SPL; noise-burst amplitude: 74 dB SPL; PSTHs taken over 170-s sampling time). Increasing values of b correspond to increasing phase lead. A: Correlation functions taken over the first 25 ms of the response to the noise burst. B: Correlation functions for the 70 dB sine wave stimulus, taken separately over the first 25 ms of the response to the noise burst and over the first 25 ms following that response.

response to the noise burst. Fig. 4B shows the short-term mean spike rate $\langle B \rangle$ computed over the same successive segments. Note that the time courses of $\langle B \rangle$ for the two tone amplitudes (60 and 70 dB SPL) are nearly identical. Thus, in spite of the conspicuous phase-locked response in Fig. 2B, the short-term mean spike rate (in response to the noise burst) was not affected by the tone, another indication of nearly linear response to the tone itself. Note also that the AC transfer ratios for the two levels of tone stimulus follow nearly identical trajectories (over the first 20 ms of the noise burst) still, one more indication of linear responsiveness to the tone. The consistent, conspicuous decline of AC transfer ratio in response to the noise burst, however, implies nonlinear interaction between the noise stimulus and the sinusoidal stimulus. Adaptation of the short-term mean spike rate, $\langle B \rangle$, in response to the noise burst is accompanied by an evidently concomitant decline in sensitivity to the sinusoidal stimulus. This same effect was seen consistently throughout the study, for unit after unit. It is in agreement with the data shown at the beginning of a paper by Smith et al. (1985; see their Fig. 2), who studied the time course (during adaptation) of the AC modulation of spike rate in response to sinusoidal

amplitude modulation of a tonal stimulus. It also is consistent with the data of Abbas (1981; see Fig. 4 and last 2 pages of the discussion in that paper).

Fig. 3B shows another manifestation of nonlinear interaction between the noise stimulus and the tone. For the 70 dB SPL tone, this figure shows that the phase of the correlation function, $\langle A \rangle$, computed over a 25-ms segment of the low-level noise (beginning 10 ms after the end of the noise burst) was conspicuously different from the phase of $\langle A \rangle$ computed during the noise burst. This implies that the phase of the AC response relative to the 70 dB sinusoidal stimulus was dependent on the amplitude of the concurrent noise stimulus (see Narins and Wagner (1989) for similar observations in frog auditory axons). We found this result consistently in these studies. Fig. 5 shows another example, for a unit that had a CF of 2.1 kHz and was excited by stimulus pattern B. The PSTH in Fig. 5A,B spans 25 ms centered on the end of the noise burst. The RMS amplitude of the noise burst (corresponding to the left half of the histogram) was 74 dB SPL over the 9700 Hz bandwidth, and that of the background noise (corresponding to the right half of the histogram) was 54 dB SPL. Fig. 5C shows the correlation functions, $\langle A \rangle$, taken over the first and last 10 ms, respectively, of the unsmoothed PSTH of Fig. 5A. In most units, as in those of Figs. 3 and 5, the AC response to a fixed-amplitude tone showed a marked increase in phase lag (relative to the sinusoidal stimulus) when the noise amplitude was increased; in a few, the phase lag decreased. In cat, Abbas (1981) reported consistent dependence of AC-response phase on noise level in 4 of 78 fibers, and the shift also was in the direction of increasing phase lag with increased noise amplitude.

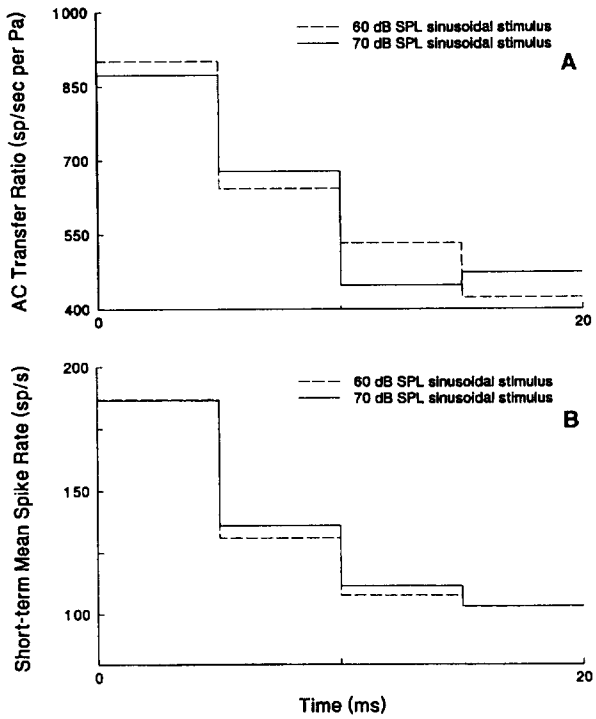

Fig. 4. AC transfer ratios (A) and short-term mean (DC) spike rates (B) for the 3.0 kHz unit of Fig. 2 during the first 20 ms of adaptation to the noise burst (again stimulus pattern B with 1-kHz tone; background noise amplitude: 54 dB SPL; noise-burst amplitude: 74 dB SPL; PSTHs taken over 170-s sampling times).

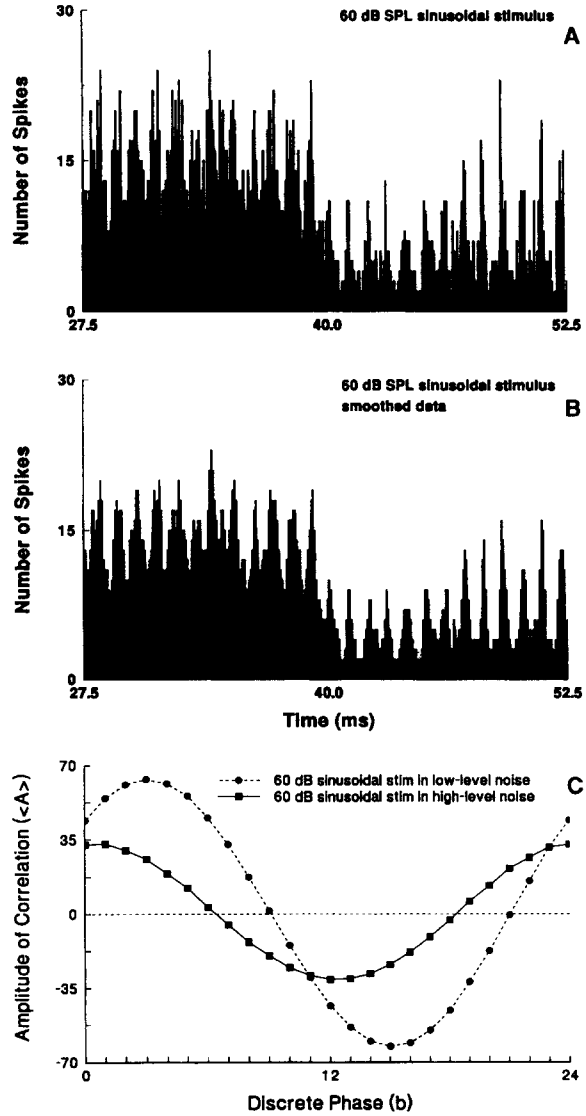

Fig. 5. Another example of the dependence of AC response phase on noise level (stimulus pattern B with 1-kHz tone; background noise amplitude: 54 dB SPL; noise-burst amplitude: 74 dB SPL; PSTH taken over 120-s sampling time). Unsmoothed (A) and smoothed (B) PSTHs for a 2.1 kHz unit. The PSTHs cover the last 12.5 ms of the response to the noise burst and the first 12.5 ms after the end of that response. The correlation functions (C) were taken separately over the first 10 ms and the last 10 ms of the PSTH of (A).

Fig. 6 shows PSTHs covering approximately the last 14 ms of the noise burst and the subsequent 36 ms of continuous background noise. Again, the RMS amplitude of the noise burst was 74 dB SPL over the 9700 Hz bandwidth, and that of the background noise was 54 dB SPL. The unit of Fig. 6A was that of Fig. 2. The amplitude of the tone

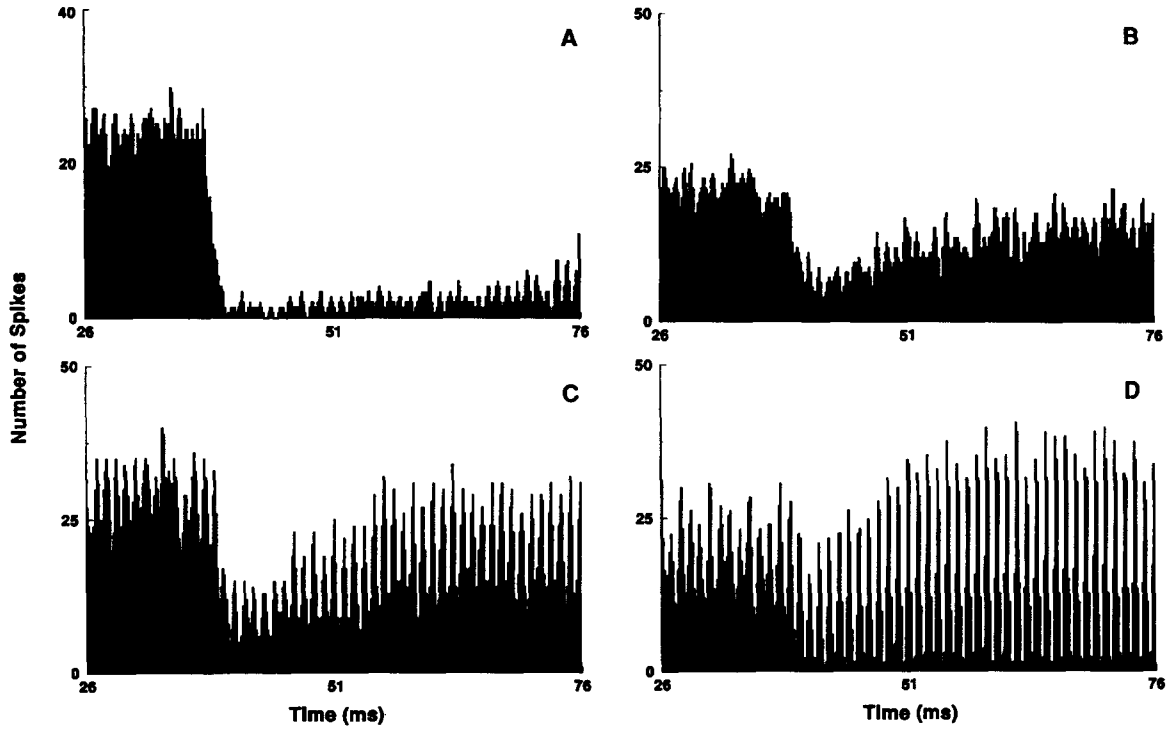

Fig. 6. PSTHs for the 3 kHz unit of Fig. 2 (A) and the 2.1 kHz unit of Fig. 5 (B–D), taken over a 50-ms segment of the 101-ms noise cycle of stimulus pattern B. The PSTHs cover the last 14 ms of the response to the noise burst and the subsequent 36 ms. For all 4 panels, the background noise amplitude was 54 dB SPL (for the 9700 Hz bandwidth), which was 20 dB below the level of the noise burst. A: tone = 1 kHz, 60 dB SPL. B–D: tone = 1 kHz, 50, 60 and 70 dB SPL, respectively. All 4 histograms were smoothed by a single convolution with the 3-bin function. Sampling times: (A) 170 s, (B) 150 s, (C) 120 s, (D) 160 s.

was 60 dB SPL. The value of $\langle A \rangle / C$ (the AC transfer ratio) taken over the first 10 ms following the noise burst (beginning at 40 ms in the figure) was 90 sp/s per Pa. Over the next 25 ms, $\langle A \rangle / C$ doubled. The background noise (54 dB SPL for the 9700 Hz bandwidth) produced a low short-term mean spike rate (4 sp/s immediately after the noise burst, increasing to 12 sp/s over the next 30 ms). Therefore, in order to be unclipped, AC responses to the tone had to be very small. The unit of Fig. 6B–D (which was the same as that of Fig. 5) was much more responsive to the background noise stimulus, and therefore allowed larger unclipped responses to tones. This unit was driven with the same noise levels as that of 6A. The tone amplitudes in 6B–D, respectively, were 50, 60 and 70 dB SPL. The AC responses (of instantaneous spike rate) to the 70 dB tone are clipped; those to the 50 and 60 dB tones are not. Fig. 7A shows $\langle A \rangle / C$ for the 60 dB tone, computed over four successive 5-ms intervals beginning at the end of the response to the noise burst (at 40 ms in Fig. 5). The 60 dB tone was selected for this plot because the AC response to the 50 dB tone was insufficient, relative to the noise, to follow accurately. Fig. 7B shows the trajectories of $\langle B \rangle$ (short-term mean spike rate) for this same unit with tones of 50 and 60 dB SPL. Both trajectories show gradual increases in $\langle B \rangle$ over time following termination of the noise burst. As was the case during the noise burst, there is a concomitant change in the AC transfer ratio, $\langle A \rangle / C$,

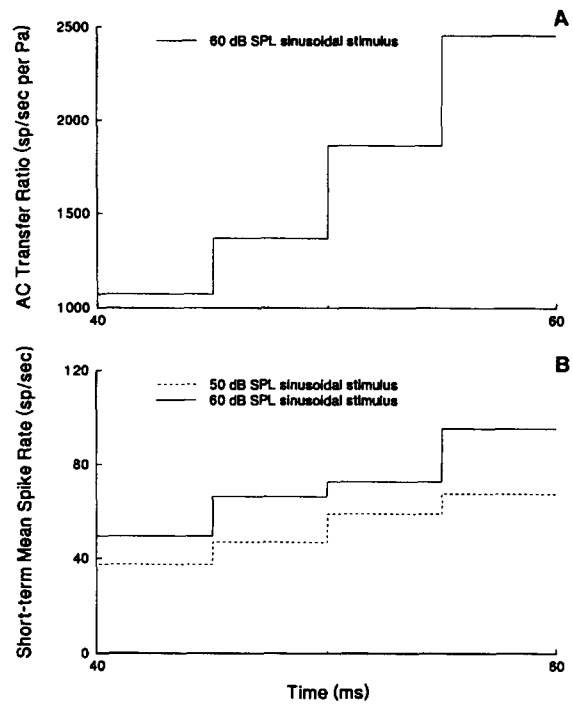

Fig. 7. AC transfer ratio (A) and short-term mean spike rates (B) for the 2.1 kHz unit of Figs. 5 and 6 during the first 20 ms of adaptation to the low-level noise (immediately after the end of the response to the noise burst). Stimulus pattern B with 1 kHz tone; background noise amplitude: 54 dB SPL; noise-burst amplitude: 74 dB SPL.

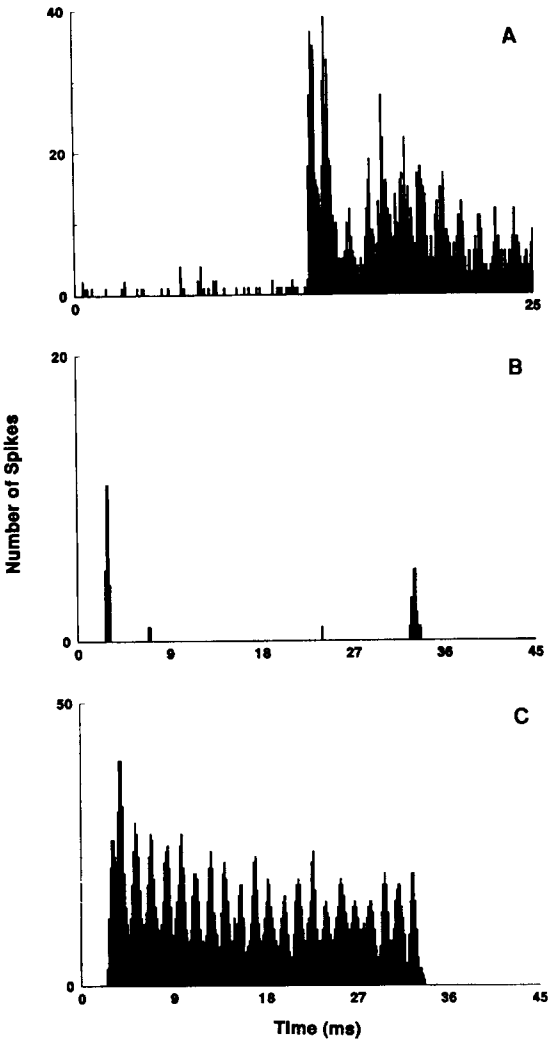

Fig. 8. PSTHs for low-spontaneous-rate units with high CFs. The tone stimulus produced conspicuous AC modulation of spike rate when the noise was present, but not when the noise was absent. A: Response (unsmoothed PSTH) of an 11.5 kHz (CF) unit to stimulus pattern A with a 1 kHz tone. The response to the noise burst begins midway across the PSTH. B and C: Responses (smoothed PSTHs) of an 8 kHz (CF) unit to stimulus pattern C. B: 700 Hz tone burst alone. C: Noise and tone bursts applied together. Sampling times: (A) 130 s; (B) 26 s; (C) 84 s.

again implying a nonlinear interaction between the noise stimulus and the tone. There also appears to be a nonlinear component in the response to the tone itself evidenced by the upward shift in the trajectory of $\langle B \rangle$ when the tone amplitude was increased by 10 dB.

With respect to the effects of adaptation (to the turning on and off of the noise burst) on AC responsiveness, our protocol yielded results consistent with those of Figs. 2–7 for all units with CFs ranging from 1 to 7 kHz. Such results were visible, however, only over limited ranges of noise amplitudes and sinusoidal stimulus amplitudes; and those ranges varied markedly from unit to unit. The amplitude of the noise burst had to be sufficient to produce a strongly adapting response. The amplitude of the tone had to be sufficient to produce measurable phase-locked response but not so large as to produce a clipped response or to pre-adapt the unit so that it no longer produced a strongly adapting response to the noise burst. When background noise was used, its amplitude had to be sufficiently large to produce a short-term mean spike rate that was high enough to provide a background that would allow unclipped phase-locked response to the tone. On the other hand, the protocol failed if the background noise was so large that it pre-adapted the unit and eliminated the strongly adapting response to the noise burst.

We examined only 3 units with CFs higher than 7 kHz. All three exhibited very low spontaneous spike rates. In each case, in the absence of the noise burst, the low-frequency tone (amplitude up to 75 dB SPL) failed to produce a conspicuous AC component of instantaneous spike rate; but in the presence of the noise burst that same tone yielded a large AC component. A steady-state version of this effect was reported by Rhode et al. (1978) for the squirrel monkey (see left side of their Fig. 7A). Two examples for the gerbil are given in Fig. 8. The response of an 11.5 kHz (CF) unit to stimulus pattern A is shown in Fig. 8A. The amplitude of the noise burst was 84 dB SPL (for the 9700 Hz bandwidth) and that of the tone was 75 dB SPL. Note that strong phase-locked response to the tone occurred only during the time of the noise burst, even though the tone was on throughout the time represented by the histogram. A similar effect can be seen in Fig. 2B, which shows a sharp decline in the amplitude of AC modulation of instantaneous spike rate when the noise level dropped. Fig. 8B,C shows responses of a unit with CF of 8 kHz (35 dB SPL threshold); the stimulus was presented in pattern C, with 0 rise and fall times for the tone burst. For Fig. 7B the stimulus comprised a 700 Hz (73 dB SPL) tone alone. Spike responses occurred at the onset and termination of the tone burst, but virtually no response occurred during the plateau. For Fig. 8C, a noise burst (0.5-ms rise and fall times) with RMS amplitude of 51 dB SPL (9700 Hz bandwidth) was added in synchrony with the same tone burst, leading to robust phase-locked response to the latter. The response to the tone-burst onset is still apparent. The PSTH in Fig. 8A shows a conspicuously nonmonotonic profile of adaptation and AC responsiveness. This sort of nonmonotonic profile was not uncommon, but the time scales of the bounce varied.

In most units when the amplitude of the tone was large, the short-term mean spike rate in response to the tone and noise together were greater than the responses to either alone. When the frequency of the tone was close to CF, however, we occasionally found evidence of 2-tone rate suppression. The unit of Fig. 9 is an extreme example. It had a CF of 800 Hz (estimated off-line from REVCOR analysis) and a threshold of approximately 20 dB SPL at 1 kHz. Stimulus pattern B was used. For all 4 panels, the sampling time was 180 s; the RMS amplitude of the

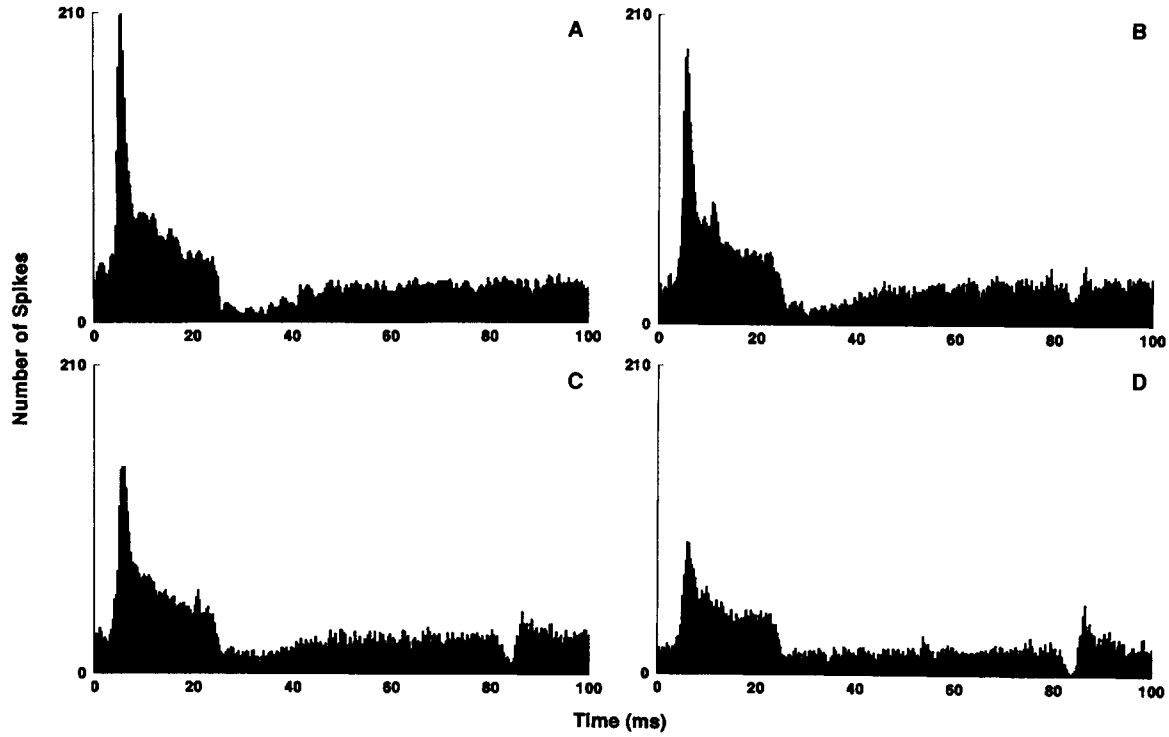

Fig. 9. PSTHs showing adaptation and suppression in a unit with CF of 800 Hz, in response to stimulus pattern B with noise burst duration of 20 ms. Each PSTH shows the response over the entire 101-ms stimulus cycle. The amplitude of the background noise was 64 dB SPL for the 9700 Hz bandwidth; the noise amplitude during the burst was 84 dB SPL. A: Response to noise alone. B–D: Responses to noise plus tone. The tone levels were 55, 60 and 65 dB SPL for (B), (C) and (D), respectively. Sampling time was 180 s for each PSTH. Histograms were smoothed by a single convolution with the 3-bin function.

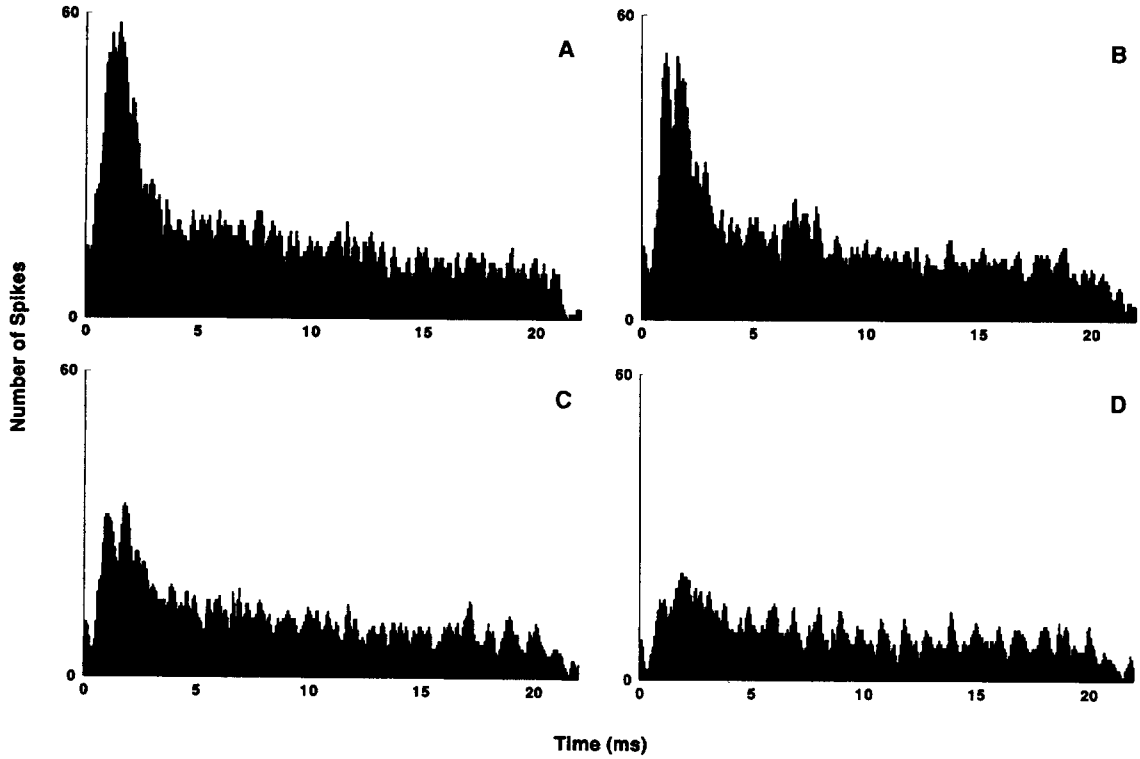

Fig. 10. PSTHs of the data of Fig. 9 with higher temporal resolution. Again, the response to noise alone is shown in (A), and the tone levels were (B) 55, (C) 60 and (D) 65 dB SPL. Sampling time again was 180 s for each PSTH. Histograms were smoothed by a single convolution with the 3-bin function.

background noise was 64 dB SPL (9700 Hz bandwidth), and that of the noise burst was 84 dB SPL. With no tone present (Fig. 9A) the response to the noise burst (beginning at ≈ 5 ms on the PSTH) was primary-type with an exaggerated initial peak. Fig. 9B–D show the effects of adding a 1.0 kHz tone at levels of 55, 60 and 65 dB SPL. These tone levels were repeated in various orders, yielding the same results. The mean spike rate taken over the entire stimulus period in the absence of tone was approximately 50 spikes/s. The mean rate remained nearly constant at this level when tones of 55 and 60 dB SPL were added, but for tones of 65 dB SPL and more the mean rate dropped conspicuously (e.g., to 27 spikes/s at 70 dB SPL). One might take this to be evidence of 2-tone rate suppression. In this case, it is the mean spike rate in response to noise that is reduced by an added tone. On the other hand, when the tone was terminated for 1 ms (at ≈ 83 ms on the time axis of Fig. 9), the response to the background noise was diminished further. This latter effect has not been reported with 2-tone rate suppression but is commonly seen associated with adaptation (adaptation to a tone burst can produce momentary reduction in response to a background noise stimulus when the tone burst is terminated). As is true with adaptation, the effect was more pronounced as the level of the tone was increased. Thus the patterns in the PSTHs of Fig. 9 appear to reflect properties commonly associated with 2-tone rate suppression, and properties commonly associated with adaptation. We found this same effect, in varying degrees, in 7 of the 8 units that had CFs estimated between 1 and 1.5 kHz. When the tone resumed (after being off for 1 ms), the response of the unit of Fig. 9 initially was greater than the response to the noise alone. We observed this effect in only one other unit, which had a CF of approximately 1.5 kHz. The fact that a 1-ms pause in the tone could lead to a response as pronounced as that in Fig. 9D was surprising to us.

In Fig. 10 we examine the data of Fig. 9 with higher temporal resolution through the noise burst. In Fig. 10B, the amplitude (A) of the AC modulation of instantaneous spike rate clearly is largest during the initial peak of the response to the noise burst. This result was found commonly in these experiments, for units of all CFs tested. Thus A often increased above its background level when the noise burst began. This effect is illustrated in Fig. 11, where we show PSTHs for the units of Fig. 2 and Fig. 9, but with increased time resolution (12 bins/ms) and centered about the transition from low- to high-level noise (stimulus pattern B). The histogram in Fig. 11A was smoothed by a single convolution with our 3-bin function. That in Fig. 11B was not smoothed. In both cases, A increased conspicuously when the noise burst began. For the first cycle or first few cycles of the tone after the response to the noise burst ended, A typically was nearly the same or slightly less than its value near the end of the noise burst (e.g., see Fig. 5). Returning to Fig. 10, with the unit undergoing 2-tone rate suppression, one can see that as the amplitude of the tone increased, the phase-locked response to the tone during the initial peak of the response to the noise burst became increasingly suppressed, while the phase-locked responses later in the noise burst grew in amplitude.

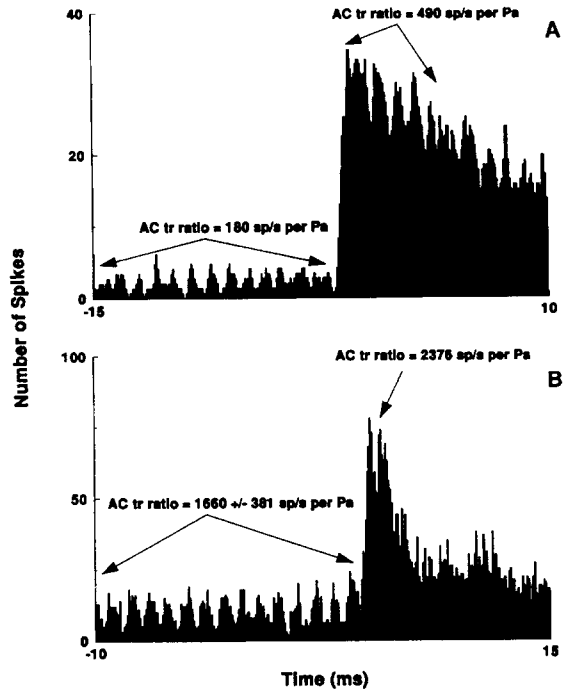

Fig. 11. PSTHs showing AC transfer ratio before and after the transition from low- to high-level noise during application of stimulus pattern B. A: Same unit and stimulus conditions as in Fig. 2A, histogram smoothed by single convolution with the 3-bin function. B: Same unit and stimulus conditions as in Fig. 10B, histogram not smoothed.

4. Discussion

In the present study, during the periods in which the amplitudes of two stimulus components (noise and sine wave) were constant, the stimulus waveform, $S(t)$, could be described as

$$S(t) = v(t) + C\sin[2\pi f_0 t] \quad (10)$$

where C is constant and f_0 is the frequency of the tone, and v has a Gaussian distribution with zero mean (i.e., with the mean amplitude of positive excursions being the same as that of negative excursions) and constant standard deviation (RMS value). One could imagine this composite stimulus as a random signal (with Gaussian amplitude distribution) whose mean is varying sinusoidally. We took the instantaneous spike-rate response to $S(t)$ to be described by Eq. 3. Changes in A while the RMS noise amplitude and the tone amplitude remain constant should be largely reflective of changes in responsiveness of the auditory periphery itself and largely independent of the

shuffling or phase-smearing effects inherent in the phase locking to one stimulus in the presence of another (i.e., synchrony suppression: Johnson, 1978; Javel, 1981; Greenwood, 1986). Consistent with the findings of Abbas (1981), in every situation in which A and B could be evaluated we found that they had nearly parallel trajectories over time after a sudden change in noise level (e.g., see Figs. 4 and 7). The nearly parallel trajectories of A and B correspond to vector strength (r in Eqs. 5 and 6) that is nearly constant through the course of adaptation. Thus, while the AC responsiveness (measured as $\langle A \rangle / C$, the AC transfer ratio) changed markedly during adaptation to the noise bursts, the vector strength did not (see also the discussion in Abbas, 1981). The results of our experiments show that when the amplitude of the tone is sufficiently small, the AC responsiveness can be strongly dependent on the recent history (measured in terms of milliseconds) of the RMS value (ν_{RMS}) of the noise, $v(t)$, while being nearly independent of the tone amplitude; e.g., see Fig. 4A.

The conventional definition of a linear function includes two properties: additivity $[f(x_1 + x_2) = f(x_1) + f(x_2)]$ and homogeneity $[f(K_1 x_1) = K_1 f(x_1)]$. Therefore, if $f[S(t)]$ is a linear function, then

$$f[K_1 S_1(t) + K_2 S_2(t)] = K_1 f[S_1(t)] + K_2 f[S_2(t)] \quad (11)$$

The total stimuli applied in this study comprise two components (noise and sine wave) that would lead to easily separable responses in a system behaving linearly. In response to a sine wave beginning at time t_1,

$$S_1(t) = C \sin[2\pi f_0 (t - t_1)] \quad t \geq t_1$$

$$S_1(t) = 0 \quad t < t_1 \quad (12)$$

a linearly behaving system would produce a sine wave component at the same frequency plus a transient component, $g_1(t)$

$$f[S_1(t)] = A \sin[2\pi f_0 (t - t_1) + \theta] + g_1(t - t_1) \quad t \geq t_1$$

$$f[S_1(t)] = 0 \quad t < t_1 \quad (13)$$

In response to noise beginning at t_2,

$$S_2(t) = v(t) \quad t \geq t_2$$

$$S_2(t) = 0 \quad t < t_2 \quad (14)$$

the linearly behaving system would produce a random component, $N(t)$, plus a transient component, $g_2(t)$,

$$f[S_2(t)] = N(t) + g_2(t - t_2) \quad t \geq t_2$$

$$f[S_2(t)] = 0 \quad t < t_2 \quad (15)$$

In response to both stimuli applied together, the linearly behaving system would produce a response of the form

$$f[S_1(t) + S_2(t)] = A \sin[2\pi f_0 (t - t_1) + \theta] + g_1(t - t_1) + N(t) + g_2(t - t_2) \quad t \geq t_1, \ t \geq t_2 \quad (16)$$

Thus, by the conventional definition of linearity, the changes of A that we found in response to sudden changes in ν_{RMS} correspond to nonlinearities in the auditory pathway between the outer ear canal and the auditory nerve fiber. These nonlinearities can be separated into two classes: (1) those whose effects appeared very rapidly when the RMS noise level was suddenly changed (as in Fig. 8), and (2) those whose effects unfolded more slowly after a change of RMS noise level, as described in the preceding paragraph. The latter are analogous to automatic gain control in electronic amplifiers.

There are many ways that such nonlinearities might arise. To aid our own interpretation of the rapid nonlinear relationship implied by the data, we invoked a spike-trigger model based on the following assumptions. (1) The generator potential, V_G, in the vicinity of the spike trigger, is an affine function of the stimulus, $S(t)$,

$$V_G(t) = G\{C \sin[2\pi f_0 t + \theta'] + v(t)\} + V_{GO} \quad (17)$$

where G is a multiplicative factor and V_{G0} is the resting value of the generator potential. (2) The threshold, V_T, of the spike trigger is constant. (3) The instantaneous spike rate is directly proportional to the probability that the instantaneous amplitude of V_G exceeds V_T. Because we are not including any spike-trigger dynamics or any dependence of instantaneous spike rate on the recent history of firing, the model is a time-varying Poisson process (see caveat in Introduction). Our purpose in employing it here is to gain qualitative understanding.

Define a normalized variable, x,

$$x = \frac{V_G - V_{GO}}{G v_{RMS}} \quad (18)$$

so that

$$x(t) = \frac{C}{v_{RMS}} \sin[2\pi f_0 t + \theta'] + v(t) OVER v_{RMS}$$

$$x_T = \frac{V_T - V_{GO}}{G v_{RMS}} \quad (19)$$

If the amplitude (C) of the tone were zero, then the probability density function for the instantaneous amplitude of x would be a normalized Gaussian curve, $n(x)$, with $\sigma_x = 1$ (see Fig. 12A):

$$n(x) = \frac{1}{\sqrt{2\pi}} e^{-\frac{x^2}{2}} \quad (20)$$

The instantaneous spike rate in our model would be directly proportional to the area, $1 - N(x_T)$, under the curve to the right of the normalized threshold, x_T.

$$1 - N(x_T) = \int_{x_T}^{\infty} n(x)\,dx \tag{21}$$

For nonzero values of C, the probability density function for the instantaneous amplitude of x will be a normalized Gaussian curve with its mean varying sinusoidally about zero, described by the function

$$n(x - x_m) = \frac{1}{\sqrt{2\pi}} e^{-\frac{(x-x_m)^2}{2}}$$

$$x_m(t) = \frac{C}{v_{RMS}} \sin[2\pi f_0 t + \theta'] \tag{22}$$

i.e., the Gaussian curve in Fig. 12A would shift right and left in a sinusoidal fashion, without changing shape, while the threshold remained fixed. The area to the right of x_T (and thus the instantaneous spike rate in the model) would undergo periodic modulation at the frequency of the tone. For a tone of fixed, small amplitude, the amplitude of this periodic modulation will depend markedly on v_{RMS} (see Fig. 12B). It is clear from Fig. 12B that as long as v_{RMS} is less than $(V_T - V_{G0})/G$ (i.e., $1/x_T < 1$), then a sudden *increase* of v_{RMS} will produce an immediate *increase* of the AC modulation of instantaneous spike rate in response to the tone, as we observed in the data.

With the spike-trigger model of the previous paragraph, as long as the center of the Gaussian curve remains to the left of the threshold, then the maximum increase in instantaneous spike rate during a shift of the mean to the right of zero will be greater than the decreases in spike rate during a shift of the same amplitude to the left of zero. To test the data for the presence of nonlinearity with these properties, we used a simple algorithm (suited to our spread-sheet approach) for estimating the positive and negative peak amplitudes of AC modulation of instantaneous spike rate. The first step constructed sequences of peak-to-trough and trough-to-peak differences in the sinusoidal modulation of the PSTH:

$$A_R(k) = (-1)^k X_{a+km/2} + (-1)^{k+1} X_{a+(k+1)m/2} \tag{23}$$

where X_i is the number of spikes in bin i; m is the number of bins per sinusoidal stimulus cycle; bin a is the first bin $(0 \le a < m)$; and the sequence is taken over successive positive integral values of k. Thus, for each

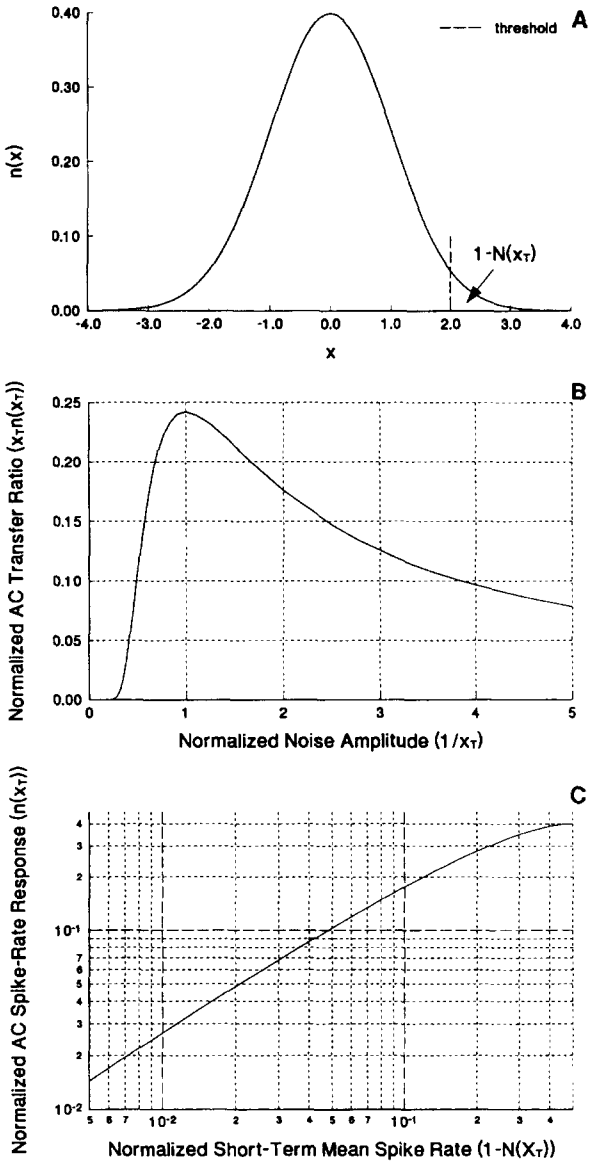

Fig. 12. A simple descriptive model of spike generation. The random variable, x, is the normalized generator potential (at a spike trigger zone); $n(x)$ is the normal (Gaussian) probability density function; the dashed line depicts the position of the threshold (x_T) along the x axis; $N(x_T)$ is the area under the curve to the left of x_T, 1-$N(x_T)$ is that to the right of x_T. The spike rate in the model is taken to be directly proportional to the value of 1-$N(x_T)$. If x is taken to be directly proportional to the stimulus (which for the experiments of this paper is described by Eq. 10), then the effect of the tone stimulus can be visualized as a horizontal, back and forth shifting of the curve in (A) while the position of the threshold is held fixed (or, alternatively, as a back and forth shifting the threshold while the position of the curve is held fixed). The corresponding modulation of the spike rate is taken to be directly proportional to the modulation of the area to the right of threshold. For small-amplitude back and forth shifts, the amplitude of the corresponding modulation would be directly proportional to the amplitude of the shifts and directly proportional to the value of $n(x_T)$. Under the normalization scheme defined in Eq. 19, with the parameters of the system fixed, $1/x_T$ is directly proportional to the rms noise amplitude, and the AC transfer ratio is directly proportional to $x_T n(x_T)$. The plot of $x_T n(x_T)$ vs. $1/x_T$ in (B) illustrates the effect of noise amplitude that emerges from the model. For small noise amplitudes, AC transfer ratio is essentially 0. When the rms noise amplitude is $(V_T$-$V_{G0})/G$ (i.e., when $x_T = 1$) the AC transfer ratio is maximum (see Eq. 19). The short-term-mean spike rate is taken to be proportional to the value of 1-$N(x_T)$. The plot of $n(x)$ vs. 1-$N(x_T)$ in (C) illustrates the near proportionality between spike-rate modulation and short-term-mean spike rate that emerges from this model under conditions of fixed noise and sine-wave amplitudes (e.g., during adaptation).

cycle of the stimulus sine wave, two terms in each sequence were generated. A different sequence was generated for each discrete value (a) of phase, and the sequence whose terms summed to the largest positive integer was selected. We took the corresponding value of a (a_{max}) to be the best match (with resolution $2\pi/m$ rad) to the phase of the sinusoidal modulation of the histogram. The next step constructed average peak positive excursions ($\langle P_p \rangle$) and average peak negative excursions ($\langle P_n \rangle$) from the short-term mean spike rate:

$$\langle P_p \rangle = \frac{1}{KN\tau}\left[\sum_{k=0}^{K-1} X_{a_{\max}+km} - \frac{1}{m}\sum_{j=1}^{mK} X_j\right]$$

$$\langle P_n \rangle = \frac{1}{KN\tau}\left[\frac{1}{m}\sum_{j=1}^{mK} X_j - \sum_{k=0}^{K-1} X_{a_{\max}+(k+1/2)m}\right] \qquad (24)$$

where N is the number of repetitions of the noise burst; τ is the time represented by each histogram bin; K is the number of cycles of (approximately) sinusoidal modulation of spike rate over which the sum is taken in a given PSTH. In each case, this was done with the raw (unsmoothed) histograms as well as with histograms that had been convolved with the 0.25, 0.5, 0.25 smoothing function. In every case, the average peak positive excursion exceeded the average peak negative excursion. For example, for the histogram in Fig. 2A, the average peak positive excursion during the noise burst was 8% greater than the average peak negative excursion. In Fig. 2B it was 13% greater. As one would expect, the differences usually were considerably greater in unsmoothed data. For the unsmoothed data corresponding to the histograms in Fig. 2A,B, the average peak positive excursions were greater than the average peak negative excursions by 29% and 41%, respectively. For the smoothed data of Fig. 6B and C, beginning at the 50-ms point (well after the end of the noise burst) and ending at 100 ms (1 ms before the onset of the subsequent noise burst), the average peak positive excursions were greater than the average peak negative excursions by 7% and 15%, respectively. The corresponding unsmoothed data yielded 6% and 51%, respectively. Because these results are *qualitatively* consistent with the model of the previous paragraph, we believe that the simplest interpretation of the rapid nonlinear relationships implied by our observations is to consider them to be attributable largely to the spike-generator threshold and to the nature of our stimuli (i.e., to the Gaussian shape of the amplitude distribution of $\nu(t)$ translated, by middle-ear and cochlea, to a similar shape of the amplitude distribution of the generator potential).

The slowly unfolding nonlinear relationships implied by the changes in A that occurred over time while stimulus parameters remained fixed, on the other hand, must reflect adjustments in the properties of the ear. The fact that, during adaptation to the noise burst, changes in AC responsiveness followed trajectories that closely paralleled those of changes in short-term mean spike rate seemed to us to impose an interesting constraint on the underlying mechanisms. In terms of the spike-trigger model of the previous paragraphs, for very small values of tone amplitude (C), A would be directly proportional to the height of the Gaussian curve, $n(x_T)$, at normalized threshold, which is a strong function of x_T. The short-term mean spike rate would be proportional to the area, $1 - N(x_T)$, under the portion of the Gaussian curve to the right of the threshold. Fig. 12C shows a plot of the relationship between these two variables (for values of normalized threshold ranging from 0 to 2.5). If the process of adaptation corresponded to a shift of x_T (while C and ν_{RMS} remained fixed), then the model would yield a concomitance between A and B that approximates direct proportionality (e.g., at the left hand edge of the curve in Fig. 12C, a change in x_T that led to a doubling of short-term mean spike rate would also lead to a 1.80-fold increase of the amplitude of AC modulation of instantaneous spike rate). A shift of x_T (in the absence of a change in ν_{RMS}), can be accomplished by any one or more of the following: (1) a shift of the threshold value, V_T, of the generator potential (i.e., a shift of the threshold of the spike generator), (2) a shift of G, the transfer relation (or 'gain') imposed by the ear, (3) a shift in the short-term mean generator potential, V_{G0} (i.e., a short-term DC component added to the generator potential). In the context of our spike trigger model, all of these shifts are equivalent (see Eq. 19) and would account equally well for the adaptation effects that we observed. Most current hypotheses regarding cochlear adaptation attribute it to depletion of synaptic reservoirs, which could directly affect both G and V_{G0} (e.g., Eggermont, 1975, 1985; Smith and Brachman, 1982; Westerman and Smith, 1988; Chimento and Schreiner, 1991). Changes in V_T would depend on spike-trigger dynamics, which so far we have ignored. According to one of the most faithful descriptive models of the spike trigger, the process of accommodation, which unfolds with time constants of the order of a few milliseconds, tends to keep the threshold at a constant distance from the generator potential (see Hill, 1936). Thus, the process of accommodation, which presumably is related to spike-trigger channel kinetics (e.g., opening of voltage-dependent potassium channels, inactivation of voltage-dependent sodium channels), also could play a role in the effects that we observed.

The behavior described in the previous paragraph for our spike-trigger model depends on the presence of noise in the generator potential. In our experiments, we injected noise as part of the external auditory stimulus. There also are many sources of noise within the ear (e.g., random thermal motion of the micromechanical structures, random emissions of synaptic transmitter, random opening and closing of ion channels, random flow of ions through channels). Thus, one might very reasonably consider $\nu(t)$ to comprise two components: one originating outside the ear and the other arising within the ear. As long as the

slope of the probability density function for the instantaneous amplitude of the generator potential (V_G) were negative at the spike-trigger threshold (V_T), then adaptation could be a consequence of any of the three shifts listed at the end of the previous paragraph. The actual shape of the density function need not be Gaussian to give qualitatively similar results. In fact, one expects the Gaussian amplitude distribution of externally applied noise to be reshaped by nonlinearities within the ear (e.g., a sigmoid nonlinearity associated with transduction, see Hudspeth and Corey, 1977).

Nevertheless, the Gaussian distribution provides a convenient vehicle for examining, qualitatively, the behavior expected from the spike-trigger model. One of the behaviors already noted is a maximum in the responsiveness to a sine-wave stimulus (measured as AC transfer ratio) when that responsiveness is plotted against the amplitude of a noise stimulus applied with the sine wave (see Fig. 12B). On the low-noise side of that maximum, the responsiveness increases with increasing noise level. This apparently paradoxical relationship is seen in our physiological data (see Fig. 8 and Fig. 11). It is similar to a phenomenon that has been called *stochastic resonance* (Balsara et al., 1991; Douglass et al., 1993; Wiesenfeld and Moss, 1995), which is being explored in amphibian ears by Narins and his colleagues (Narins et al., 1995). Stochastic resonance has been defined as a maximum in the plot of the *ratio of signal amplitude to noise amplitude in the response* against *noise amplitude in the stimulus*, with the amplitude of the stimulus sine wave held constant. We did not look for such a maximum in our physiological experiments, but the spike-trigger model predicts that it will occur. For a given bin in a PSTH, the signal amplitude can be taken to be the expected number of spikes in the presence of the sine wave stimulus less the expected number of spikes in the absence of that stimulus; and the noise amplitude can be taken to be the RMS deviation from the expected value in the absence of the sine wave stimulus. If we assume that the probability (p) of a spike occurring in a given bin of the PSTH for a given presentation of the noise burst is independent of the occurrence of spikes in that bin during previous presentations and is constant from one presentation to the next, then the number of spikes in that bin will be a random number with a binomial distribution. The RMS deviation of the spike count from its expected value (i.e., the standard deviation) will be $\sqrt{p(1-p)N}$. The expected value itself is pN. In our physiological observations, p always was small (e.g., in Fig. 2, the largest number of spikes per bin was approximately 75, and the number of noise-burst presentations was 1700, implying a value of p of the order of 0.044). In such cases (i.e., p very small), the RMS noise amplitude in a PSTH bin should be approximately equal to $\sqrt{pN}$, the square-root of the expected number of spikes in that same bin. For our trigger model with Gaussian noise, the ratio of signal amplitude to noise amplitude is maximum when

$$v_{RMS} \approx 0.61 \frac{V_T - V_{GO}}{G} \tag{26}$$

(see Fig. 13). This relationship defines the stochastic resonance point for the model (for sine-wave stimuli with very small amplitudes). Narins and his colleagues currently are searching for such a maximum in the auditory periphery itself (Narins et al., 1995).

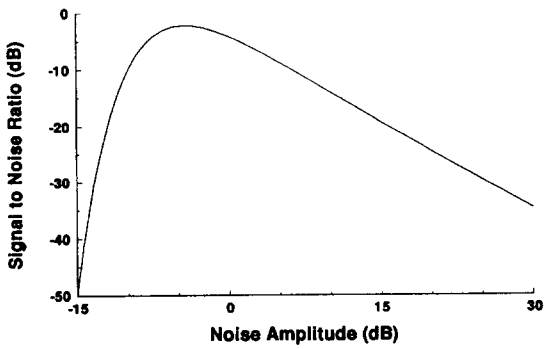

Fig. 13. Signal-to-noise ratio plotted against noise amplitude for the model of Fig. 12. Zero dB of noise amplitude corresponds to $v_{rms} = (V_T - V_{GO})/G$.

5. Conclusion

Noise impacts spike triggering in several ways. In his celebrated modeling studies, FitzHugh (1955, 1961) concluded that spike generation owes its all-or-none (threshold) properties to the presence of noise, an hypothesis corroborated subsequently by the work of Cole et al. (1970) and Clay (1976) (see MacGregor and Lewis, 1977, pp. 186–187). Stein (1970) and others (e.g., see Yu and Lewis, 1989) have shown that independent noise at the spike trigger of each member of a population of axons can counteract the effects of threshold and allow the population to code continuous signals (e.g., sine waves) in a continuous manner to signal levels well below the threshold of the individual spike trigger. This is analogous to dithering, which is employed by engineers to soften the effects of the lowest-level bit in digitally recorded waveforms. In dithering (which relies on a very high sampling rate in a single channel rather than a large number of parallel channels), added noise makes the system responsive to signal amplitudes that otherwise would be below the threshold for that last bit. The idea is not new to students of the inner ear. It was put forth, implicitly, by Lowenstein (1956) nearly 40 years ago when he concluded that spontaneously active axons, in principle, have no threshold.

In this paper, we conclude that noise, by virtue of its amplitude distribution (specifically, the shape of the probability density function for its instantaneous amplitude) also can provide interesting nonlinearities. Among other things,

it can endow a spike trigger with the ability to translate a change in the DC component of the generator potential to a change in sensitivity to small AC signals.

Acknowledgements

The research reported here was supported by the Deafness Research Foundation and the National Institute of Deafness and Communicative Disorders (Grant DC-00112). We thank Eva Hecht for help in preparing the illustrations; and we are grateful to Peter Narins for bringing the concept of stochastic resonance to our attention.

References

Abbas, P.J. (1981) Auditory-nerve fiber responses to tones in a noise masker. Hear. Res. 5, 69–80.

Anderson, D.J., Rose, J.E., Hind, J.E. and Brugge, J.F. (1970) Temporal position of discharges in single auditory nerve fibers within the cycle of a sine-wave stimulus: frequency and intensity effects. J. Acoust. Soc. Am. 49, 1131–1139.

Balsara, A., Jacobs, E.W., Ting, Z., Moss, F. and Kiss, L. (1991) Stochastic resonance in a single neuron model: theory and analog simulation. J. Theoret. Biol. 152, 531–555.

Chimento, T.C. and Schreiner, C.E. (1991) Adaptation and recovery from adaptation in single fiber responses of cat auditory nerve. J. Acoust. Soc. Am. 90, 263–273.

Clay, J.R. (1976) A stochastic analysis of the graded excitatory responses of nerve membrane. J. Theoret. Biol. 59, 141–158.

Cole, K.S., Guttman, R. and Bezanilla, F. (1970) Nerve membrane excitation without threshold. Proc. Natl. Acad. Sci. USA 65, 884–891.

Costalupes, J.A., Young, E.D. and Gibson, D.J. (1984) Effects of continuous noise backgrounds on rate response of auditory nerve fibers in cat. J. Neurophysiol. 51, 1326–1344.

Costalupes, J.A. (1985) Representation of tones in noise in the response of auditory nerve fibers in cats. I. Comparison with detection thresholds. J. Neurosci. 5, 3261–3269.

De Boer, E. and de Jongh, H.R. (1978) On cochlear encoding: potentialities and limitations of the reverse-correlation technique. J. Acoust. Soc. Am. 63, 115–135.

Dolan, D.F. and Nuttall, A.L. (1989). Inner hair cell responses to tonal stimulation in the presence of broadband noise. J. Acoust. Soc. Am. 86 1007–1012.

Douglass, J.K., Wilkens, L., Pantazelou, E. and Moss, F. (1993) Noise enhancement of information transfer in crayfish mechanoreceptors by stochastic resonance. Nature 365, 337–339.

Edwards, B.W. and Wakefield, G.H. (1993) The spectral shaping of neural discharges by refractory effects. J. Acoust. Soc. Am. 93, 3353–3364.

Eggermont, J.J. (1975) Cochlear adaptation: a theoretical description. Biol. Cybern. 19, 181–189.

Eggermont, J.J. (1985) Peripheral adaptation and fatigue: a model oriented review. Hear. Res. 18, 57–71.

Erell, A. (1988) Rate coding model for discrimination of simple tones in the presence of noise. J. Acoust. Soc. Am. 84, 204–214.

FitzHugh, R. (1955) Mathematical models of threshold phenomena in the nerve membrane. Bull. Math. Biophys. 17, 257–278.

FitzHugh, R. (1961) Impulses and physiological states in theoretical models of nerve membrane. Biophys. J. 1, 445–466.

Freedman, E.G., Ferragamo, M. and Simmons, A.M. (1988) Masking patterns in the bullfrog (*Rana catesbeiana*). II. Physiological effects. J. Acoust. Soc. Am. 884, 2081–2091.

Goldberg, J.M. and Brown, P.B. (1969) Response of binaural neurons of dog's superior olivary complex to dichotic tonal stimuli: some physiological mechanisms of sound localizations. J. Neurophysiol. 32, 613–636.

Greenwood, D.D. (1986) What is 'synchrony suppression'? J. Acoust. Soc. Am. 79, 1857–1872.

Hill, A.V. (1936) Excitation and accommodation in nerve. Proc. Roy. Soc. Lond. B119, 305–355.

Hudspeth, A.J. and Corey, D.P. (1977) Sensitivity, polarity, and conductance change in the response of vertebrate hair cells to controlled mechanical stimuli. Proc. Natl. Acad. Sci. USA 74, 2407–2411.

Javel, E. (1981) Suppression of auditory nerve responses. I. Temporal analysis, intensity effects and suppression contours. J. Acoust. Soc. Am. 69, 1735–1745.

Johnson, D.H. (1978) The relationship of post-stimulus time and interval histograms to the tuning characteristics of spike trains. Biophys. J. 22, 413–430.

Johnson, D.H. (1980) The relationship between spike rate and synchrony in responses of auditory-nerve fibers to single tones. J. Acoust. Soc. Am. 68, 1115–1122.

Lewis, E.R. and Henry, K.R. (1989) Cochlear nerve responses to waveform singularities and envelope corners. Hear. Res. 39, 209–224.

Lowenstein, O. (1956) Peripheral mechanisms of equilibrium. Br. Med. Bull. 12, 114–118.

MacGregor, R.J. and Lewis, E.R (1977) Neural Modeling. Plenum, New York.

Narins, P.M. (1987) Coding of signals in noise by amphibian auditory nerve fibers. Hear. Res. 26, 145–154.

Narins, P.M., Bendix, J.H. and Moss, F. (1995) Effect of temperature on signal-to-noise ratio in the auditory nerve of the frog. ARO Abstr. 18, 174.

Narins, P.M. and Hillery, C.M. (1983) Frequency coding in the inner ear of anuran amphibians. In: Hearing — Physiological Bases and Psychophysics, R. Klinke and R. Hartmann (Eds.), Springer, Heidelberg, pp. 70–76.

Narins, P.M. and Wagner, I. (1989) Noise susceptibility and immunity of phase locking in amphibian auditory-nerve fibers. J. Acoust. Soc. Am. 85, 1255–1265.

Palmer, A.R. and Russell, I.J. (1986) Phase-locking in the cochlear nerve of the guinea-pig and its relation to the receptor potential of inner hair-cells. Hear. Res. 24, 1–15.

Perkel, D.H., Gerstein, G.L. and Moore, G.P. (1967) Neuronal spike trains and stochastic point processes. I. The single spike train. Biophys. J. 7, 391–418.

Rhode, W.S., Geisler, C.D. and Kennedy, D.T. (1978) Auditory nerve fiber responses to wide-band noise and tone combinations. J. Neurophysiol. 41, 592–704.

Selby, S.M. (1975) Handbook of Tables for Mathematics. CRC Press, Boca Raton, FL.

Siebert, W.M. (1968) Stimulus transformations in the peripheral auditory system. In: Recognizing Patterns, P.A. Kolers and M. Eden (Eds.), MIT Press, Cambridge, MA, pp. 104–133.

Smith, R.L. and Brachman, M.L. (1982) Adaptation in auditory-nerve fibers: a revised model. Biol. Cybern. 44, 107–120.

Smith, R.L., Brachman, M.L. and Frisina, R.D. (1985) Sensitivity of auditory-nerve fibers to changes in intensity: a dichotomy between decrements and increments. J. Acoust. Soc. Am. 78, 1310–1316.

Stein, R.B. (1970) The role of spike trains in transmitting and distorting sensory signals. In: The Neurosciences, F.O. Schmitt (Ed.), Rockefeller University Press, New York, pp. 597–604.

Teich, M.C., Turcott, R.G. and Lowen, S.B. (1991) The fractal doubly stochastic Poisson point process as a model for the cochlear neural spike train. In: Mechanics and Biophysics of Hearing, P. Dallos, C.D.

Geisler, J.W. Matthews, M.A. Ruggero, and C.R. Steele (Eds.), Plenum, New York, pp. 354–361.

Westerman, L.A. and Smith, R.L. (1988) A diffusion model of the transient response of the cochlear inner hair cell synapse. J. Acoust. Soc. Am. 83, 2266–2276.

Wiesenfeld, K. and Moss, F. (1995) Stochastic resonance and the benefits of noise: from ice ages to crayfish and SQUIDs. Nature 373, 33–36.

Winslow, R.L. and Sachs, M.B. (1988) Single-tone intensity discrimination based on auditory-nerve rate responses in backgrounds of quiet, noise, and with stimulation of the crossed olivocochlear bundle. Hear. Res. 35, 165–190.

Young, E.D. and Barta, P.E. (1986) Rate responses of auditory nerve fibers to tones in noise near masked threshold. J. Acoust. Soc. Am. 79, 426–442.

Yu, X. and Lewis, E.R. (1989) Studies with spike initiators: linearization by noise allows continuous signal modulation in neural networks. IEEE Trans. Biomed. Eng. 36, 36–43.